scientific reports

Check for updates

OPEN

Development of a self-assembling multimeric Bann-RBD fusion protein in *Pichia pastoris* as a potential COVID-19 vaccine candidate

Ozi Jumadila[1], Muhammad Dzul Fakhri[1], Adam Darsono[2], Fernita Puspasari[1], Sari Dewi Kurniasih[1,6], Fifi Fitriyah Masduki[1,5], Keni Vidilaseris[3], Ihsanawati Ihsanawati[1], Anita Artarini[4,5], Marselina Irasonia Tan[2,5], Ernawati Arifin Giri-Rachman[2,5] & Dessy Natalia[1,5]✉

The development of an affordable and accessible vaccine platform is essential for achieving global and long-term protection against COVID-19 and other emerging viral diseases. In this study, we developed a multimeric fusion protein comprising the SARS-CoV-2 receptor-binding domain (RBD) and the β-annulus (Bann) from the tomato bushy stunt virus (TBSV) as a potential subunit vaccine candidate. Molecular modeling of Bann-RBD revealed a 60-mer structure with the RBD displayed on its outer surface. The Bann-RBD gene was constructed and overexpressed in *Pichia pastoris* X-33. SDS-PAGE analysis of the purified Bann-RBD showed a protein band at 45 kDa, corresponding to monomeric glycosylated Bann-RBD. Peptide mapping analysis using LC-MS/MS confirmed that the expressed Bann-RBD was consistent with the designed protein fusion. The Bann-RBD protein was observed to spontaneously self-assemble into spherical nanocapsids with a diameter of approximately 50 nm. Antigenicity studies demonstrated that the purified Bann-RBD was strongly recognised by monoclonal human anti-SARS-CoV-2 spike-S1 IgG antibodies. Immunogenicity studies revealed that Bann-RBD elicited a robust humoral immune response in BALB/c mice, generating potent neutralising antibodies. Collectively, these findings suggest that the recombinant Bann-RBD produced in *Pichia pastoris* X-33 is a promising candidate for the development of a COVID-19 vaccine.

Keywords COVID-19, Multimeric protein, RBD, Subunit vaccine, β-annulus

Abbreviations

RBD	Receptor binding domain
Bann	β-annulus
TBSV	Tomato bushy stunt virus
COVID-19	Coronavirus disease 2019
SARS-CoV-2	Severe acute respiratory syndrome coronavirus 2
PHEIC	Public health emergency of international concern
ACE2	Angiotensin-converting enzyme 2
VLP	Virus like particle
HPV	Human papillomavirus

[1]Biochemistry and Biomolecular Engineering Research Division, Faculty of Mathematics and Natural Sciences, Institut Teknologi Bandung, Jl. Ganesa No. 10, Bandung 40132, Indonesia. [2]School of Life Sciences and Technology, Institut Teknologi Bandung, Jl. Ganesa No. 10, Bandung 40132, Indonesia. [3]The Molecular and Integrative Biosciences Research Programme (MIBS), Faculty of Biological and Environmental Sciences, University of Helsinki, Biocenter 1/ Viikinkaari 9, 00014 Helsinki, Finland. [4]Laboratory of Pharmaceutical Biotechnology, School of Pharmacy, Institut Teknologi Bandung, Jl. Ganesa No. 10, Bandung 40132, Indonesia. [5]Biosciences and Biotechnology Research Centre, Institut Teknologi Bandung, Jl. Ganesa No. 10, Bandung 40132, Indonesia. [6]Sari Dewi Kurniasih is deceased. ✉email: dessynatalia@itb.ac.id

HbsAg	Hepatitis B surface antigen
RGNNV	Red-spotted grouper nervous necrosis virus
MSAs	Multiple sequence alignments
VIPERdb	Virus particle explorer database
LC-MS/MS	Liquid chromatography tandem mass spectrometry
ELISA	Enzyme linked immunosorbent assay
HSA	Human serum albumin
DLS	Dynamic light scattering
LB	Luria bertani
YPD	Yeast extract peptone dextrose
BMGY	Buffered glycerol-complex medium
BMMY	Buffered methanol-complex medium
PBS	Phosphate-buffered saline
BSA	Bovine serum albumin
HRP	Horse radish peroxidase
TMB	3,3',5,5'-tetramethylbenzidine
OD	Optical density

The ongoing health concern of Coronavirus Disease 2019 (COVID-19), caused by the transmission of severe acute respiratory syndrome coronavirus 2 (SARS-CoV-2), is no longer classified as a Public Health Emergency of International Concern (PHEIC)[1]. Nonetheless, there remains a need for affordable, effective, and accessible vaccine, particularly in middle-income countries, to attain self-sufficiency in vaccine production and ensure long-lasting protection[2]. Among the various COVID-19 vaccine candidates, protein subunit vaccines are prominently developed, with 59 out of 183 vaccine candidates in the clinical trial phase[3]. Several COVID-19 protein subunit vaccines that have been approved include Novavax[4], Zifivax (ZF2001)[5], COVAX-19[6], MVC-COV1901[7], and Corbevax[8]. Protein subunit vaccines offer several advantages, such as their ability to stimulate a robust humoral immune response, non-infectious nature, and less side effect. However, these vaccines necessitate adjuvants to enhance the immune response, require substantial production capacity, need for cold chain transfer and storage[9].

SARS-CoV-2 enters host cells by attaching its surface transmembrane spike (S) protein to ACE2 receptors in the respiratory mucosa of the host. The receptor binding domain (RBD), a crucial component of the spike-S1 protein, directly binds to the ACE2 receptor during the initial phase of virus internalization[10]. The RBD serves as a potential antigen capable of eliciting neutralization antibodies that can impede the virus interaction with angiotensin-converting enzyme 2 (ACE2) receptor[11,12]. Multiple epitopes within the RBD contribute to this neutralization process, prompting investigations into both monomeric and oligomeric forms of RBD[13]. The use of RBD as a vaccine target faces challenges due to its limited immunogenicity resulting from its small molecular size and potential existence in various forms, such as monomers, dimers, or trimers. Several strategies to address these limitations, include increasing the antigen size such as by fusing the RBD with an Fc domain or by multimerization[13]. The multimeric presentation of antigens boosts B cell activation through receptor crosslinking, significantly enhancing humoral immune responses[14].

Various studies indicate that dimeric, trimeric, and multimeric RBD forms generate higher levels of neutralizing antibodies compared to the monomeric RBD[15–17]. For example, yeast-derived dimeric RBD exhibited greater efficacy in inducing neutralizing antibody production, exhibiting higher affinity for the hACE2, and inducing stronger antigen-specific germinal center responses than monomeric RBD[15]. Similarly, trimeric RBD adjuvanted with Alum-3 M-052 induces a significantly higher neutralizing antibody response and shows to a 500-fold greater affinity for ACE2 compared to monomeric RBD[16]. Moreover, the covalent coupling of multimeric RBD to Lumazine Synthase from *Brucella abortus* (BLS) further enhances the immunogenicity of RBD[17].

Comparative studies of various genetic fusions of RBD to different nanoscaffolds, such as foldon, ferritin, lumazine synthase, and β-annulus (Bann) peptide, were delivered as DNA plasmids and recombinant proteins[18]. Among these RBD modifications, the Bann-fused RBD delivered as a DNA plasmid demonstrated the most significantly enhanced antibody titers and virus neutralization, while triggering a minimal immune response compared to larger scaffolds[18]. The Bann-fused RBD exhibited prolonged presence within lymph nodes and induced the strongest viral neutralization during immunization with a recombinant protein in mice immunization[18]. However, previous study did not succeed in demonstrating the formation of multimeric proteins. Therefore, in this study, a different strategy was employed to modify the RBD with the Bann peptide, adhering to the characteristics of the N- and C-terminus regions of the Bann peptide[19].

This study introduces a vaccine candidate utilizing a protein subunit approach, where the SARS-CoV-2 RBD protein is engineered to form multimers by fusing it with the Bann protein derived from the TBSV. The Ile69-Ser92 motif of the Bann peptide in the TBSV capsid plays a role in the creation of a dodecahedral internal skeleton. This peptide has demonstrated spontaneous self-assembly, forming a multimeric protein or virus-like particle (VLP) with diameters ranging from 30 to 50 nm[20]. The Bann peptide serves as a scaffold known for generating multimeric proteins[19]. Modification of the C-terminus regions of the Bann peptide with antigen allows for the display of multiple proteins and particles on the VLP's surface[19]. In this study, we modified the C-terminus of Bann by adding the SARS-CoV-2 RBD, which facilitated the creation of a multimeric Bann-RBD protein that presents the RBD on the surface of the multimeric protein structure. By repeating the RBD protein on the surface of the multimeric Bann-RBD protein, it allows for the presentation of multiple RBD epitopes, thereby inducing an optimal immune response. The Bann peptide has a sequence composition that is hypo-immunogenic[18]. Due to its smaller size compared to the RBD, the Bann peptide is shielded within the Bann-RBD structure, further enhancing its hypo-immunogenic properties.

VLPs displaying a repetitive pattern of antigen on their surface aim to simulate a natural infection, eliciting an optimal immune response[21]. Conjugated antigens, attached to scaffolds via genetic fusion or chemical conjugation, which can lead to self-assembly and specific orientation of the antigens, demonstrate enhanced immunogenicity compared to free antigens[22]. We genetically fused the Bann with the SARS-CoV-2 RBD which was designed to expose the RBD on the outer surface of the nanocapsid. Therefore, the creation of a multimeric Bann-RBD in this study was directed to enhance its immunogenicity.

Yeast expression system for therapeutic recombinant protein presents a cost-effective and attractive production platform, including for vaccine antigens. Strains such as *Saccharomyces cerevisiae*, *Hansenula polymorpha*, and *Pichia pastoris* are commonly used. Various VLP proteins produced in *S. cerevisiae* yeast, such as hepatitis B surface antigen (HbsAg) for hepatitis B, HPV16 and 18 protein for papillomavirus, Gag protein for HIV-1/AIDS, rotavirus VP2, VP6, and VP7 for rotavirus, and varicella-zoster virus gE VLP for chickenpox[23]. Other VLP protein for vaccine expressed in *P. pastoris*, such as DENV envelope protein for dengue, hepatitis C core protein (HccAg) from hepatitis C virus for hepatitis C, HPV16L1/18L1 from papillomavirus type 16 for papilloma, P1 and 3CD proteins of EV71 for hand, foot, and mouth disease (HFMD)[23]and HbsAg from hepatitis B virus[24]. *H. polymorpha* is used for the expression of several VLP protein, such as HPV52L1 from HPV for papilloma, envelope glycoprotein E1 for hepatitis, membrane integral small surface protein (dS) of the duck hepatitis B fused with virus antigen infecting animals for infectious disease in animal, and PCV2b protein for postweaning multisystemic wasting disease (PMWS) in pigs[23]. Among these yeasts, *P. pastoris* has become popular due to its cost-effectiveness, capability to properly fold proteins in the endoplasmic reticulum, and its ability to secrete recombinant proteins into the external environment. It also produces minimal endogenous secretory proteins, achieves high yields with glycosylation patterns similar to those of mammalian cells, and offers easy recombinant protein purification. Additionally, it is regarded as a unique host for subunit vaccine expression, significantly impacting the expanding medical biotechnology market[25]. The expression of SARS-CoV-2 RBD in *P. pastoris*, when compared to RBD expressed in HEK-293T mammalian cells, demonstrated correct folding and similar stability[26].

This study presents the development of a fusion protein comprising Bann and RBD as a potential COVID-19 subunit vaccine candidate. The Bann-RBD fusion protein was genetically expressed in *P. pastoris*. Here, we present details of protein production, purification, physicochemical characterization, antigenicity assessment, and immunogenicity evaluation.

Results

Bann-RBD protein modeling

In this study, we employed protein structural modeling to validate the self-assembly of the fusion Bann-RBD (225 amino acids) into a multimeric protein. Given that the C-terminus of the Bann peptide is positioned on the exterior of the artificial capsid[27], we designed a fusion protein with the RBD attached to the C-terminus of Bann peptide. The trimeric subunit of Bann was based on the structure of TBSV coat protein (PDB ID: 2TBV)[28,29]. Bann peptide was predicted forming a C3-symmetric and self-assembled into nanocapsules[20]. We specifically used the SARS-CoV-2 RBD Delta variant, corresponding to residues R328-K528 of the SARS-CoV-2 Delta variant RBD protein (GenBank UAL04647.1)[30] (Fig. S1).

The molecular model of Bann-RBD was constructed by assembling twenty trimeric subunits into a 60-mer, based on the icosahedral arrangement observed in the TBSV viral capsid[18]. Monomeric Bann-RBD and trimeric Bann structures were predicted using ColabFold v1.5.2 with Alphafold2 and Mmseqs2[31]. Bann-RBD 60-mer was generated by the Oligomer Generator in the Virus Particle Explorer database (VIPERdb) v3.0[32].

We hypothesize that the Bann-RBD monomer can self-assemble into a multimeric Bann-RBD structure in aqueous solution. The resulting VLP of multimeric Bann-RBD protein model revealed a 60-mer protein consisting of twenty trimeric Bann-RBD, with Bann forming the core and RBD displayed on the molecular surface (Fig. 1). This structural model offers valuable insights into the potential organization and arrangement of the Bann-RBD in its multimeric state.

Epitope prediction of Bann-RBD and its interaction with B cell and T cell receptors

We perform an in silico study of Bann-RBD epitope againts B cell receptors using BepiPred-2.0, an immunoinformatic prediction software on http://tools.iedb.org/bcell/[33]. Epitope prediction results with a score above 0.5 and amino acid residue lengths between 5 and 25 are considered. Bann-RBD showed seven epitopes which could bind antibodies (Figure S2): "RFPNITNLCPF"; "VYAWNRKRISNCVA"; "ASFSTFK"; "QIAPGQTGKIAD"; "VIAWNSNNLDSKVG"; "ERDISTEIYQAGSKPCNGVEGF"; and " GFQPTNGVGYQPYR" (Table S1). These seven epitopes are shown multiple in each monomer in different conformations within the multimeric Bann-RBD structure, which is predicted to generate an optimal immune response.

The in silico prediction of the Bann-RBD epitope againts T cell receptors was performed by predicting peptide binding to MHC class I and MHC class II molecules using the IEDB website (http://tools.iedb.org/main/tcell/)[34,35]. For MHC class I epitope prediction, a cutoff score of 0.7 was applied, resulting in 22 epitopes with lengths of 9–10 amino acid residues (Table S2). For MHC class II epitope prediction with a cutoff score of 0.7 and an optimal amino acid length of 15 residues, 5 epitopes were identified (Table S3).

The molecular model of Bann-RBD was docked with the human MHC I and MHC II structures to evaluate the effect of Bann-RBD modification on the interaction between RBD and the T cell receptor. The T cell epitopes of Bann-RBD, involved in antigen-T cell receptor interactions, were analyzed using the High Ambiguity Driven protein-protein DOCKing (HADDOCK 2.4) web server[36,37]. HADDOCK 2.4 is an information-driven, flexible docking tool used for studying protein-protein interactions. The binding affinity of Bann-RBD with human MHC I and MHC II was subsequently determined using the PROtein binDIng energy prediction (PRODIGY)

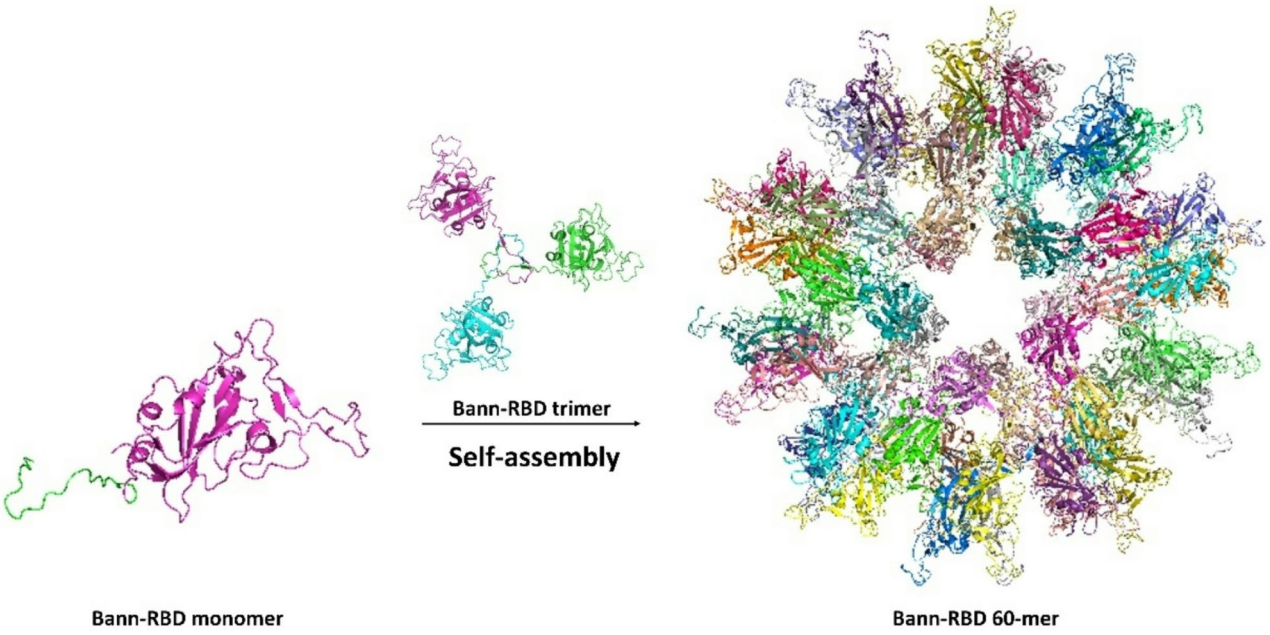

Fig. 1. Molecular modeling of Bann-RBD. The Bann-RBD monomer consists of two colors, Bann peptide in green color and RBD in magenta. Bann-RBD monomer undergoes self-assembly into a multimeric 60-mer Bann-RBD structure, with a transitional state characterized by a trimeric structure. Each color in the Bann-RBD 60-mer represents a different monomer. The structural models of the Bann-RBD monomer, trimer, and 60-mer, were visualized using PyMOL version 1.8.0.1.

web server[38,39]. PRODIGY predicts binding affinity in protein-protein complexes through a contact-based approach.

The Bann-RBD–MHC I complex exhibited a binding affinity (Δ*G*) of -14.4 kcal/mol, while the Bann-RBD–MHC II complex had a binding affinity of – 11.6 kcal/mol. All binding affinity values were negative, indicating that the interactions between Bann-RBD and T cell receptors are relatively strong and energetically favourable.

Expression and characterization of Bann-RBD protein

In our quest to develop a subunit protein-based vaccine platform and investigate the potential of the Bann peptide from the TBSV capsid to enhance SARS-CoV-2 RBD immunogenicity through multimerization, we engineered fusion peptide combining Bann and RBD of SARS-CoV-2 Delta variant. The design of the Bann and RBD fusion in this study is distinct from previous approaches[18]. Here, we modified the Bann peptide by attaching the RBD protein to its C-terminus, based on the natural orientation of Bann, where the C-terminus faces outward artificial capsids[19]. We then fused the gene encoding Bann with the SARS-CoV-2 RBD Delta variant and cloned it into pPICZαA plasmid for expression in *P. pastoris* X-33. A His-6x tag was added to the C-terminus of the RBD protein for protein purification. The plasmid map of pPICZαA containing the Bann-RBD fusion gene is presented in Figure S3.

The expressed protein was purified using Ni-NTA affinity chromatography. SDS-PAGE analysis of the purified Bann-RBD showed a molecular weight of approximately 45 kDa (Fig. 2a). The molecular weight of Bann-RBD was significantly higher than the theoretical molecular weight of 27.84 kDa (including the hexahistidine tag) determined by ProtParam, Expasy[40]. This differences suggest the presence of post-translational modification, specifically glycosylation. To confirm the presence of glycosylation, Bann-RBD was digested with the Endo-H_f enzyme, a fusion of endoglycosidase H and maltose-binding protein, to remove high mannose N-glycans from glycosylated protein. SDS-PAGE analysis of the deglycosylated Bann-RBD showed a molecular weight of approximately 28 kDa, closely aligned with its theoretical value (Fig. 2a). This result provides strong evidence supporting the existence of glycosylation in the Bann-RBD expressed in *P. pastoris* X-33.

To further confirm that the expressed protein contains both Bann and RBD, peptide mapping of glycosylated Bann-RBD was performed using controlled proteolysis followed by LC-MS/MS analysis. The result shows that sequence coverage was high, at approximately 88.26%, confirming that the amino acid sequence expressed in *P. pastoris* X-33 aligns with our designed peptide construct. (Fig. 2b). The peptide fragment 20–43 is likely undetected due to glycosylation at Asn28 and Asn40. Fragment 150–154 are not observed as it is too small and falls below the analytical detection limit.

The size distribution analysis from the Dynamic Light Scattering (DLS) experiment, conducted in an aqueous solution, revealed that Bann-RBD underwent self-assembly in a 10 mM Tris-HCl buffer at pH 7.4 and 25 °C, forming a multimeric protein structure. The size of the resulting multimeric Bann-RBD was determined to be 50.06 ± 20.57 nm, with the entire distribution comprising 100% of these multimeric structures (Fig. 2c). This

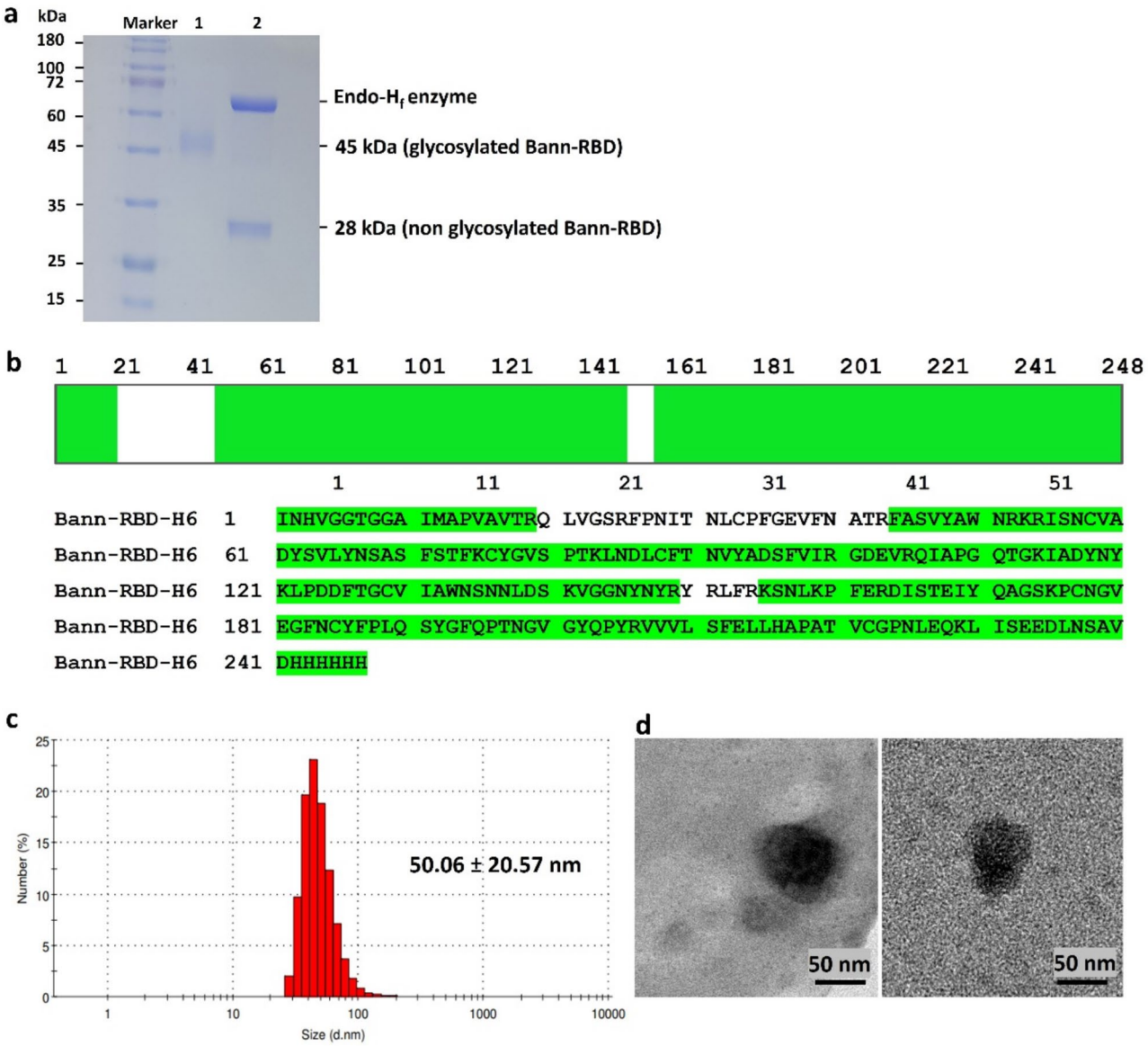

Fig. 2. Bann-RBD protein characterization. (**a**) Purified Bann-RBD treated with Endo-H_f indicating the presence of glycosylation on the Bann-RBD protein. M: protein marker; 1: purified Bann-RBD; 2: Bann-RBD treated with Endo-H_f. (**b**) Peptide mapping analysis using LC-MS/MS confirms that the expressed Bann-RBD protein sequence matches the intended design. Peptides highlighted in green indicate the regions that were successfully identified. (**c**) Bann-RBD multimer size assessment by DLS (analysis by number). (**d**) TEM image of Bann-RBD multimer. Both DLS and TEM assessments indicate that the Bann-RBD multimeric protein has a size of approximately 50 nm.

data provides valuable insights into the self-assembly properties and size characteristics of Bann-RBD under the specified condition.

Transmission Electron Microscopy (TEM) analysis was conducted to validate the size of the protein as determined by the DLS experiment. The TEM experiment focused on Bann-RBD in a 10 mM Tris-HCl buffer at pH 7.4. The results revealed the presence of spherical assemblies with an approximate size of 50 nm (Fig. 2d). Further optimization with a higher protein concentration is needed to enhance particle uniformity and structural consistency. This TEM analysis aligns with the DLS findings, providing a complementary and corroborative assessment of the size characteristics of the self-assembled Bann-RBD protein structures in the specified buffer conditions. The combined results from DLS and TEM contribute to a more comprehensive understanding of the protein's structural features.

Antigenicity study of Bann-RBD

The in vitro interaction of the purified Bann-RBD protein with specific antibodies was evaluated through an indirect enzyme-linked immunosorbent assay (ELISA). The results showed that the interaction between Bann-

RBD and human anti-SARS-CoV-2 spike-S1 IgG antibodies was nearly three times stronger than that of the monomeric RBD (Fig. 3). Conversely, human serum albumin (HSA), used as a negative control, showed no reactivity.

Immune response analysis in mice

To assess the immune response, mice were immunized with Bann-RBD supplemented with Alhydrogel and CpG ODN class C adjuvants. Two booster immunizations were administered at three-week intervals following the initial immunization (Fig. 4a). Blood samples were collected prior to and after 7, 14, and 21 days post primary immunization, as well as 21 days after the first and second booster doses.

An immunogenicity study of Bann-RBD adjuvanted with Alum-CpG revealed a remarkable humoral immune response in BALB/c mice. IgG antibody levels began to rise 14 days post-prime vaccination and were significantly enhanced 21 days after the first booster ($P < 0.0001$) in both male and female mice (Fig. 4b). Notably, the immune response increased more significantly in female mice at 14 days ($P < 0.0001$) and 21 days post-prime vaccination ($P < 0.0001$), whereas male mice exhibited a lower antibody response at 14 days ($P = 0.045$) and a modest increase at 21 days post-prime vaccination ($P = 0.004$).

Antibody-antigen interactions were evaluated using commercial SARS-CoV-2 spike-S1 protein (Fig. 4c). The results revealed that the IgG antibodies induced by three doses of Bann-RBD-Alum-CpG in mice showed a significantly higher interaction with the S1 antigen compared to the negative control sera. Additionally, IgG antibodies from female mice exhibited a stronger interaction with the S1 antigen than those from male mice.

Detection of anti-SARS-CoV-2 neutralizing antibodies

An angiotensin-converting enzyme 2 (ACE2) competitive enzyme immunoassay was performed to quantify the neutralizing antibodies (NAbs) in mice sera vaccinated with Bann-RBD, adjuvanted with alhydrogel and CpG. The results demonstrated significantly elevated levels of anti-SARS-CoV-2 NAb in both male and female mice (Fig. 5).

In contrast, the negative control group, consisting of mice vaccinated with either alhydrogel alone or alhydrogel-CpG, showed no detectable anti-SARS-CoV-2 NAb. Serum from male mice exhibited slightly lower levels of SARS-CoV-2 NAb compared to females. However, in the group of mice injected with adjuvanted Bann-RBD, one male and one female mice sera exhibited lower levels of neutralizing antibodies compared to the others, despite exhibiting high immunogenicity against Bann-RBD in previous assay. Variability in neutralizing

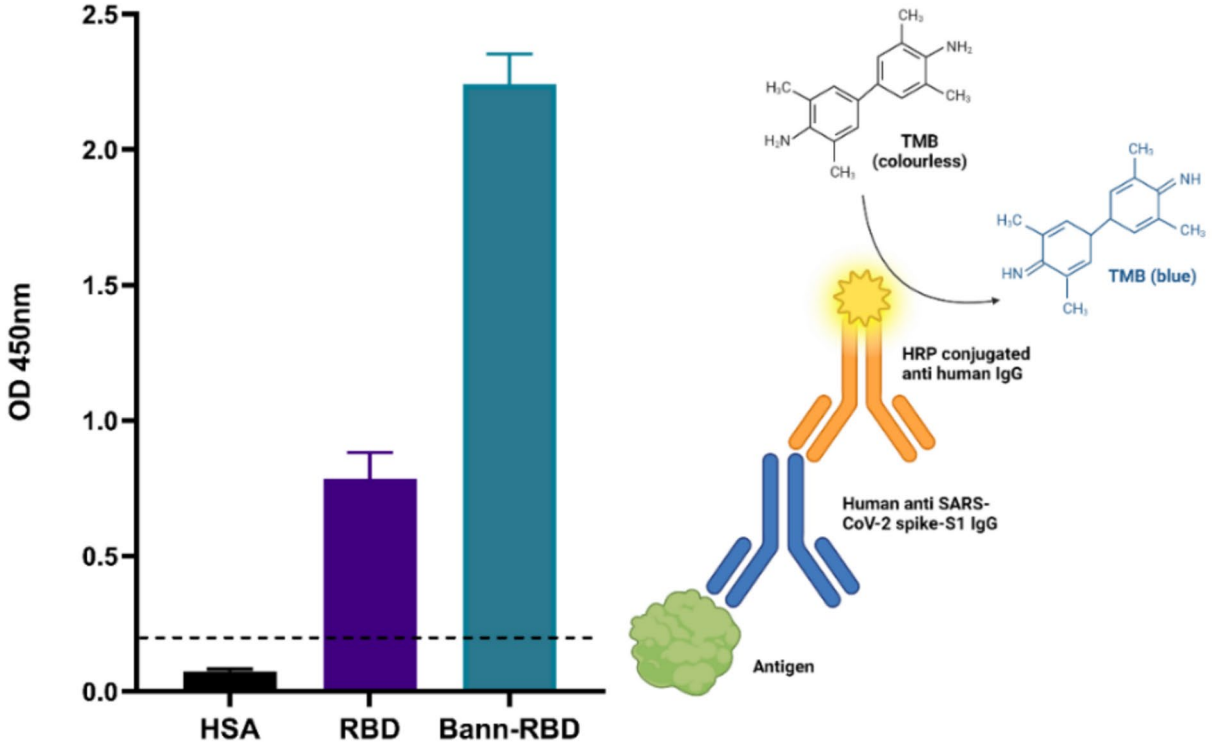

Fig. 3. Antigenicity study of Bann-RBD. Interaction of human anti-SARS-CoV-2 spike-S1 IgG antibody to Bann-RBD (blue) and RBD (purple). HSA as negative control (black). The Bann-RBD protein exhibited approximately three times higher interaction with human anti-SARS-CoV-2 spike-S1 IgG antibody compared to unmodified RBD.

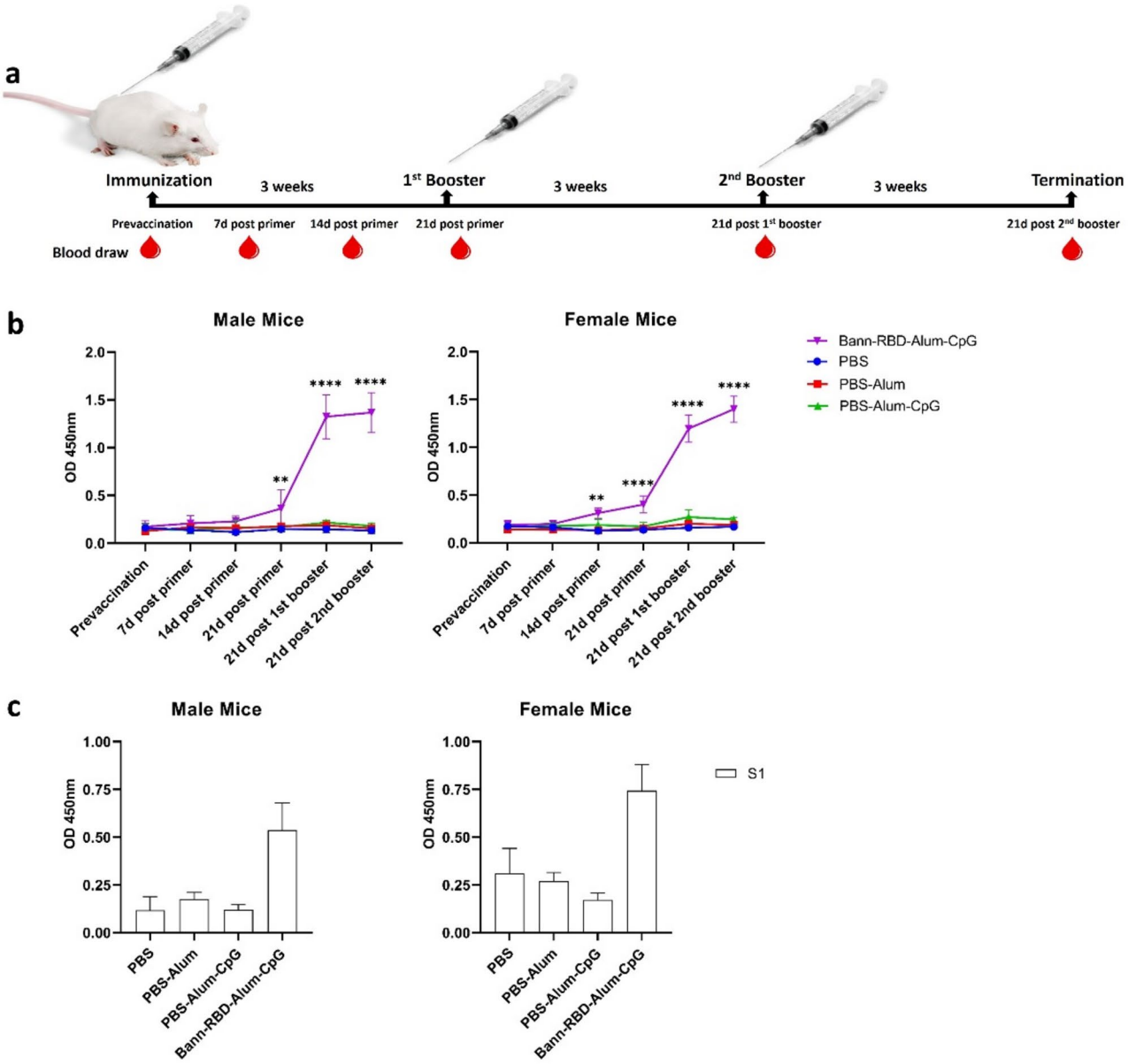

Fig. 4. Immune response analysis. (**a**) Mice immunization schedule with Bann-RBD. Bann-RBD injections were administered three times at 21-day intervals. (**b**) Humoral immune responses against Bann-RBD SARS-CoV-2 in male and female mice. The immune response increased significantly following the first booster dose. (**c**) Mice IgG antibody interaction with commercial SARS-CoV-2 spike-S1 antigen. Bann-RBD is capable of inducing antibodies that strongly interact with the S1 protein. Mice sera was diluted to 1:1000. $^{*}p = 0.045$, $^{**}p = 0.004$, $^{****}p < 0.0001$.

responses, based on epitope-mapping studies, suggests that monoclonal antibodies targeting the top of the RBD exhibit strong competition with ACE2 binding and show highly potent neutralizing activity. In contrast, antibodies targeting the side surfaces of the RBD do not compete effectively with ACE2, leading to a less potent neutralizing response[41]. Overall, the majority of mice vaccinated with Bann-RBD demonstrated high levels of SARS-CoV-2 NAb.

Preliminary study of Bann-RBD toxicity and safety

A toxicity study of the Bann-RBD protein sequence was conducted in silico using ToxinPred2 with a hybrid approach, combining scores from machine learning (RF), MERCI, and BLAST. The ML score was 0.34, the MERCI score was 0, the BLAST score was −0.5, and the hybrid score was −0.16. Overall, the protein toxicity prediction indicated that Bann-RBD protein is non-toxin.

Body weight assessments showed no adverse effects of Bann-RBD injection, the mice's body weight increases each week (Figure S5). Physical examination revealed no signs of edema (swelling) or erythema (redness) at the injection site. Body temperature remained normal after vaccination with an increase less than 1 °C (Table

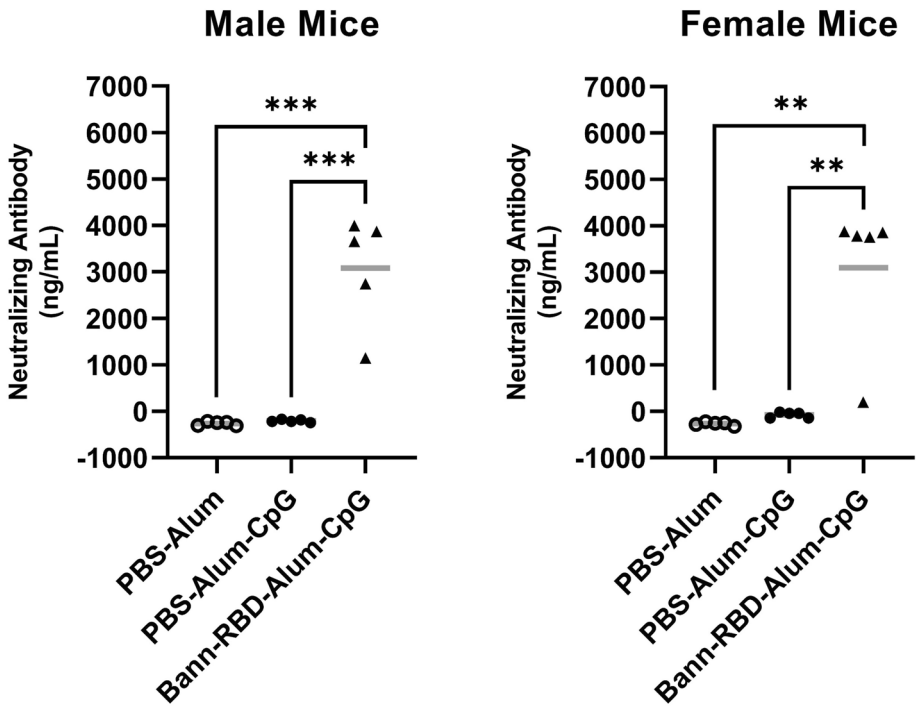

Fig. 5. In vitro assay of anti-SARS-CoV-2 neutralizing antibody in mice sera: The level of anti-SARS-CoV-2 NAbs in mice sera significantly increased after the second booster of Bann-RBD, compared to the control group. Significant differences are indicated by asterisks (Two-way ANOVA using Tukey's multiple comparisons test, $^{**}p < 0.01$, $^{***}p < 0.001$).

S4), suggesting that Bann-RBD did not induce fever. Further hematological analyses and histopathological examination will be required to assess the toxicity of Bann-RBD.

Discussion

The RBD of SARS-CoV-2 based vaccine candidate has demonstrated strong neutralization capabilities and efficacy in protecting against SARS-CoV-2 infection[12,42]. Multimeric forms of RBD have shown higher immunogenicity compared to their monomeric counterparts[43,44]. One approach to generating nanostructure vaccines involves fusing RBD to a scaffold domain. Various scaffolds have been explored in previous studies, including foldon (RBD-foldon-RBD), ferritin (RBD-ferritin), and lumazine synthase (RBD-AaLs) to create multimeric proteins[18].

Bann peptide from TBSV that consists of 24-mer has a unique feature in its ability to self-assemble into a nanocapsid[20]. Furthermore, this capsid can be functionalized by encapsulating guest molecules inside and decorating the outer surface with guest molecules by connecting additional sequences to the Bann peptide[45]. This versatile characteristic of the Bann peptide opens up possibilities for the incorporation of antigens from other pathogens, enhancing its potential as a platform for vaccine design and other applications.

A previous study showed the RBD protein fused with the Bann peptide that expressed in mammalian cells did not undergo self-assembly into multimeric proteins; instead, it maintained a monomeric state[18]. This could be due to an inappropriate fusion protein construct, RBD-Bann, where the RBD is attached to the N-terminal region of the Bann peptide, which is known to be oriented toward the interior of the capsid[27].

In our efforts to develop a subunit protein-based vaccine platform and explore the capability of the Bann peptide to boost RBD immunogenicity through multimerization, we designed fusion peptides that combine Bann and RBD protein with a new construct. Our recent study used a different construct as before, where the RBD protein is attached to the C-terminal region of the Bann peptide, which orients it toward the exterior of the capsid[19]. This new construct is expected to form a Bann-RBD multimer that displays the RBD protein on the exterior surface of the multimeric protein structure.

The self-assembly of Bann-RBD multimer was investigated using protein molecular modeling analysis. The results showed that the fusion of Bann and RBD peptides has the capacity to self-assemble into a 60-mer Bann-RBD structure. In this multimeric protein model, the RBD peptides were positioned on the exterior of the multimeric Bann peptide. The higher number of RBD peptides displayed on the outside of the multimeric protein is predicted to efficiently mask the Bann peptide, reducing its self-immunogenicity[18]. The interaction among the RBD peptides located on the exterior of the multimeric protein is suggested to contribute to the stability of multimeric Bann-RBD. This structural information provides valuable insights into the potential design principles for optimizing the immunogenic properties of the Bann-RBD vaccine candidate.

The epitope is a crucial region that enables host immune cells to recognize a specific pathogen, also known as antigenic determinant[46]. The in silico epitope analysis of Bann-RBD identified the epitopes and furthermore we located the seven epitopes on the stucture of Bann-RBD multimer as shown in Figure S2. Three epitopes "VIAWNSNNLDSKVG", "ERDISTEIYQAGSKPCNGVEGF", and "GFQPTNGVGYQPYR" are located on the surface of the Bann-RBD multimer structures, making them more accessible to specific antibodies. Epitopes "VYAWNRKRISNCVA", "QIAPGQTGKIAD", and "ERDISTEIYQAGSKPCNGVEGF" contain key epitopes for monoclonal antibody (mAb) binding, "VYAWN", "VRQIAP", and "YQAGSTP"[47]. The epitope "VYAWN is suggested as a natural linear epitope and is highly conserved across different SARS-CoV-2 strains. The epitope "VRQIAP" is a neutralizing epitope and exhibits cross-reactivity between SARS-CoV-2 and SARS-CoV[47]. The epitope "YQAGSTP" neutralizing epitope located in the receptor-binding motif (RBM). This epitope overlaps with ACE2-binding residues and exhibits variability among different SARS-CoV-2 strains[47]. Moreover, we uncovered additional immunodominant epitopes, "RFPNITNLCPF" and "ASFSTFK" overlapped with the epitope that reportedly inducing humoral immunity in mice[48].

T cells recognize peptide epitope that bind to specific class I or II major histocompatibility complex MHC molecules. MHC class I-restricted epitopes typically consist of 8–10 amino acid residues and are presented on the surface of CD8 + T cells for recognition, whereas MHC class II-restricted epitopes are generally 13–17 residues in length and are recognized by CD4 + T cells[49]. Cellular immunity analysis was performed using an in silico approach, which identified 22 epitopes on the Bann-RBD protein associated with MHC class I binding (Table S2) and five epitopes associated with MHC class II binding (Table S3). We acknowledge the limitations of our experiment. To improve the reliability of our research, further T-cell immune response experiments will be essential in providing a more comprehensive understanding of the cellular immunity induced by Bann-RBD. The in silico study of Bann-RBD interaction with the T cell receptor showed a negative binding affinity value, indicating a strong and stable interaction. The Bann-RBD-MHC I interaction was slightly weaker than RBD-MHC I, whereas the Bann-RBD-MHC II interaction was stronger than RBD-MHC II.

The production of Bann-RBD as vaccine candidate in the yeast expression system was chosen for its ability to yield a high quantity of protein and simplify the purification process. Several studies have demonstrated that yeast serves as a more scalable and cost-effective expression system for RBD production compared to mammalian cells[15,26,50]. The *P. pastoris* system utilized in this study offers several advantages. It allows for proper folding of proteins in the endoplasmic reticulum and facilitates their secretion by utilizing a peptide signal for external release. Furthermore, the *P. pastoris* expression system is known for its ease of purification of recombinant proteins, attributed to its limited production of endogenous secretory proteins[25]. These characteristics make *P. pastoris* an efficient and practical choice for the expression and production of the Bann-RBD vaccine candidate.

The molecular weight of the Bann-RBD protein expressed in *P. pastoris* X-33, as determined by SDS PAGE analysis, was observed to be 45 kDa. This molecular weight aligns with the monomeric RBD expressed in *P. pastoris* X-33 in prior studies[2,42,50–53]. Peptide mapping using LC-MS/MS showed that Bann-RBD expressed in *P. pastoris* X-33 was in accordance with our peptide construction.

The presence of glycosylation modification in Bann-RBD was confirmed by treated with Endo-H_f enzyme. Glycosylation introduced by *P. pastoris* enables correct protein folding, solubility, stability, and proper biological activity. Native-like glycosylation can reflect native-like protein folding and the presence of conformational epitopes. The influence of glycosylation in contributing to MHC epitopes, and in some cases hindering peptide presentation, highlights its critical role in shaping T-cell mediated immunity[54]. N-glycosylation of the SARS-CoV-2 RBD is essential for both the viral internalization into respiratory epithelial cells and for shielding the virus from neutralization[55].

In our size analysis conducted using DLS and TEM, multimeric Bann-RBD protein was successfully generated with a size of approximately 50 nm. This size is comparable to those observed in other studies involving protein and particle modifications with Bann peptide[56–59]. Modifications of Bann at the C-terminus with coiled-coil-A spikes, HSA, DNA, and ribonuclease S proteins resulted in the formation of spherical assemblies with sizes ranging from 40 to 160 nm[19]. Notably, the Bann-HSA conjugate self-assembled into spherical structures with a size range of 50–70 nm. For comparison, an enveloped viral replica composed of anionic self-assembled Bann peptides with a cationic lipid bilayer, equipped with a SARS-CoV-2 S protein, has a size of approximately 100 nm[60]. DLS and TEM analysis of Bann-RBD confirmed the formation of Bann-RBD multimers but were insufficient to validate the molecular model of the Bann-RBD structure. Therefore, further experimental validation is necessary, using techniques such as X-ray crystallography or cryo-EM, to confirm the degree of multimerization and the arrangement of the Bann-RBD multimer protein. This information contributes to our understanding of the self-assembly characteristics of the Bann-RBD protein and its potential application in vaccine development.

In examining the antigenicity of the modified Bann-RBD protein, an indirect ELISA was conducted using human anti SARS-CoV-2 spike-S1 IgG antibody. Bann-RBD expressed in *P. pastoris* X-33 demonstrated an increased interaction with the specific antibody compared to unmodified RBD. This enhanced interaction suggests that the modification of RBD with the Bann peptide has adopted a proper fold. This folding allows for the presentation of multiple conformational neutralizing epitopes of RBD, which is crucial for triggering an effective immune response.

Immunogenicity study of Bann-RBD adjuvanted with Alum and CpG showed a strong humoral immune response in BALB/c mice. COVID-19 vaccine formulation with the addition of TLR9 agonist CpG has been evaluated to promote antigen sparing and induce Th1/Th2 immune responses[61]. Bann-RBD as a vaccine candidate needs at least one booster injection to induce a strong protection. Our investigation in accordance with previous studies using Bann-RBD protein based vaccines[18]. The stronger interaction of mice IgG antibodies with the commercial SARS-CoV-2 spike-S1 antigen suggests that the Bann-RBD protein can induce antibodies that are highly recognized by the S1 antigen.

A competitive enzyme immunoassay was conducted to analyze the SARS-CoV-2 NAb by incubating mice sera with SARS-CoV-2 RBD conjugated to HRP and ACE2 receptors. The results indicated that sera from mice vaccinated with Bann-RBD-Alum-CpG have potent anti-SARS-CoV-2 neutralizing antibodies. The *P. pastoris*-expressed Bann-RBD protein, combined with CpG + Alum adjuvant, efficiently induced neutralizing antibodies (NAbs) against SARS-CoV-2 and its variants[42]. This study has certain limitations, as we were unable to conduct neutralizing antibody assays using a direct pseudovirus approach. Future quantitative pseudovirus neutralization assays will be needed to evaluate the efficacy of Bann-RBD as a vaccine candidate.

Our preliminary toxicity assessments of the Bann-RBD protein conducted in silico using ToxinPred2 indicated that Bann-RBD is a non-toxin protein. This data supported by body weight measurement. Each group of mice showed consistent weekly weight gain, in line with the standards established by Jackson Laboratories[62] Preliminary safety study of Bann-RBD injection to BALB/c mice indicated that Bann-RBD did not result any edema or erythema. Body temperature measurement after Bann-RBD injection confirm a slight elevation of less than 1 °C or within the healthy range of BALB/c mice[63]. We acknowledge the limitations of this study, particularly the need for more comprehensive toxicological and safety assessments of Bann-RBD, including hematological analyses and histopathology examination of various organs.

The advantage of Bann-RBD as a vaccine lies in its multiple RBD displays on the Bann-RBD antigen, which mimics the natural infection process of the virus. These studies support that *P. pastoris*-Bann-RBD emerged as a promising vaccine candidate.

Conclusion

Protein structural modeling showed the generation of multimeric Bann-RBD, presenting as a 60-mer structure with Bann forming the core and RBD decorating the surface of the multimeric protein. The synthesis of the Bann-RBD gene and its integration into *P. pastoris* X-33 were successfully accomplished. Extracellular expression of Bann-RBD was achieved, and the protein was isolated from the growth medium, followed by purification. Bann-RBD treated with Endo-H_f enzyme confirmed the glycosylation of the expressed protein. DLS and TEM analyses indicated the generation of multimeric Bann-RBD with diameters of approximately 50 nm. Antigenicity studies of the purified Bann-RBD protein demonstrated a strong interaction with monoclonal human anti SARS-CoV-2 spike-S1 IgG antibody. Adjuvanted Bann-RBD protein based vaccines with Alum and CpG showed a significant humoral immune response in mice. This study suggested that the recombinant Bann-RBD synthesized in *P. pastoris* X-33 holds promise as a candidate for the development of a COVID-19 vaccine.

The genetic fusion of Bann-RBD, as explored in this study, represents an early stage in vaccine development. Further research is required, including comprehensive toxicology and safety assessments, detailed efficacy evaluations, long-term immune response characterization, and additional neutralization assays using pseudovirus. Nevertheless, the Bann-RBD multimeric protein subunit vaccine holds promise as a potential vaccine candidate. This platform could also be adapted for other emerging viral diseases by modifying its antigenic component. The multimeric molecular model presented in this study provides a scientific foundation for advancing multimeric protein-based vaccines. Overall, this research contributes to ongoing efforts to improve the versatility, efficiency, and speed of vaccine development in response to emerging diseases.

Materials and methods

Materials

All chemicals utilized in the study were procured from various suppliers, including Fermentas (Maryland, USA), Difco Laboratories (New Jersey, USA), Promega (Madison, USA), Stratagene (La Jolla, USA), and SMOBIO (Taiwan). Synthetic genes were obtained from Genscript (USA), and oligonucleotide primers were synthesized at Macrogen (Singapore). These sources contributed to the acquisition of the necessary reagents and genetic materials for the experimental procedures conducted in the research.

Microorganism, plasmid, and growth medium

Escherichia coli TOP10F' was employed for gene cloning purposes, while *P. pastoris* X-33 served as the host for gene expression. The pGEM-T easy vector (Promega, Madison, USA) was utilized for the cloning of PCR products, and the pPICZαA vector was employed as the expression vector in the study. These specific strains and vectors played essential roles in the cloning and expression processes conducted in the research.

Luria Bertani (LB) medium was employed as the growth medium for *E. coli* TOP10F'. The composition of LB medium included 1% tripton (w/v), 0.5% yeast extract (w/v), 1% NaCl (w/v), and 1% bacto agar (w/v) for solid medium. Tetracycline was added to the solid medium as a selective agent. These components provided a suitable environment for the growth and maintenance of *E. coli* TOP10F' during the experimental procedures.

P. pastoris X-33 was cultivated in various media depending on the specific stages of the experimental process. YPD (yeast extract peptone dextrose) medium was utilized for plasmid integration, while BMGY (buffered glycerol-complex medium) and BMMY (buffered methanol-complex medium) media were employed for protein production. The antibiotics zeocin and ampicillin were used for the selection of *P. pastoris* X-33-pPICZαA-Bann-RBD, providing a selective environment for the targeted yeast strain during different phases of the study.

Bann-RBD protein modeling

The amino acid sequence of the SARS-CoV-2 RBD Delta variant (GenBank UAL04647.1) contains two mutations, L452R and T478K, and residues 328–528 were used as the template for protein modeling. Bann peptides, consisting of 24 amino acids from TBSV, were fused at the N-terminus of RBD. Protein structure modeling, including the prediction of Bann-RBD monomer and Bann trimer structures, was carried out using ColabFold v1.5.2 with AlphaFold2 and Mmseqs2 (https://github.com/sokrypton/ColabFold)[31]. For homology

searches and template identification, we utilized the MMseq2-based homology search server, which facilitated the construction of diverse multiple sequence alignments (MSAs). The trimeric structure of β-annulus (Bann) from TBSV (PDB code 2TBV) served as a template for alignment with the RBD structure using Pymol version 1.8.0.1 (www.pymol.org)[64].

The Bann-RBD structure from AlphaFold2 was oriented to the Bann 60-mer to create a Bann-RBD monomer with the same orientation as the Bann-RBD 60-mer. The Bann and RBD chains were merged using the WinCoot version 0.9.4 graphics program (https://wiki.uni-konstanz.de/ccp4/index.php/Coot) and further generated into a Bann-RBD 60-mer with the Oligomer Generator in the Virus Particle Explorer database (VIPERdb) v3.0 (https://viperdb.org/Oligomer_Generator.php)[32]. Figures and data for the Bann-RBD 60-mer were obtained from VIPERdb, a curated repository of virus capsid structures that also contains structure-derived data and various specific information. Subsequently, protein structural relaxation was performed using Relax Amber from ColabFold.

Epitope prediction of Bann-RBD and its interaction with B cell and T cell receptors

An in silico study of the Bann-RBD epitope against B cell receptors was conducted using the BepiPred 2.0 software on the IEDB website http://tools.iedb.org/bcell/[33]. T cell receptors epitope analysis was performed by predicting Bann-RBD peptide binding to MHC class I and MHC class II molecules using the IEDB website (http://tools.iedb.org/main/tcell/[34,35]

We analyzed the interaction between Bann-RBD T cell prediction epitopes and human MHC class I (PDB ID: 7zuc) and MHC class II (PDB ID: 1seb) receptors using the HADDOCK 2.4 web server (https://rascar.science.uu.nl/haddock2.4/)[36,37]. Additionally, we predicted the binding affinity of these interactions using the PRODIGY web server (https://rascar.science.uu.nl/prodigy/)[38,39].

Design, cloning, and expression of Bann-RBD

The gene encoding Bann-RBD of SARS-CoV-2 was synthesized at Genescript and inserted into the pPICZαA. The ligation of the Bann-RBD gene into pPICZαA was carried out using *EcoR*I and *Xba*I restriction sites. The pPICZαA-Bann-RBD recombinant plasmid map was provided in Figure S3.

P. pastoris X-33-pPICZαA-Bann-RBD was cultured in BMGY medium in a flask for 24 h at 30 °C with a speed of 225 rpm. Subsequently, the cultures were transferred into BMMY medium and induced with 2% (v/v) methanol every 24 h for a total period of 72 h. The cultures were then harvested, and cells were removed by centrifugation at 5,000 rpm for 15 min at 4 °C. The supernatant, which contained Bann-RBD, was separated and stored at 4 °C, while the cells were stored at -20 °C for further analysis.

Purification of Bann-RBD

Hexahistidine-tagged Bann-RBD was purified from the fermentation supernatant (FS) using Ni-NTA resin through immobilized metal affinity chromatography. The FS was concentrated by a cold methanol precipitation step with a ratio of 1:1, and the proteins were separated through centrifugation at 12,000 rpm for 10 min at 4 °C. The precipitated proteins were dissolved in buffer A (50 mM Tris-HCl, pH 8, 150 mM NaCl) before being applied to a Ni-NTA column[18]. The column was washed with buffer A supplemented with 20 mM imidazole. Elution was performed in buffer A containing 50 mM, 100 mM, 250 mM, and 500 mM imidazole, and the eluted fraction was stored at -20 °C. Purified Bann-RBD was dialyzed against a buffer of 20 mM Tris, 150 mM NaCl, pH 7.5[18], followed by another dialysis step in 10 mM Tris-HCl, pH 7.4[56]. To assess the impact of glycan on protein size, these proteins were treated with Endo-H_f, a glycosidase enzyme that removes N-glycans, and loaded onto a gel for analysis.

Peptide mapping analysis using LC-MS/MS

Proteins were separated by SDS-PAGE in reduced condition and stained with coomasie brilliant blue. Bann-RBD band was cut and gel pieces were analyzed with LC-MS/MS. This study used NCRIS-enabled Australian Proteome Analysis Facility (APAF) infrastructure. Protein samples for peptide sequencing were digested by addition of 1 µg trypsin and incubated overnight at 37 °C. Peptide samples were injected onto the peptide trap column and washed with a loading buffer. Peptides were eluted from the trap onto the nano-LC column and separated. The column eluent was directed into the ionization source of the mass spectrometer operating in peptide mode.

The mass spectrometry raw files underwent analysis using Proteome Discoverer (Thermo, Version 2.1). The searches were carried out utilizing the SequestHT search engine against a database that included the expected Bann-RBD sequence, set against the background of the *P. pastoris* database (accessed in May 2023). This approach aimed to identify and match the observed peptide sequences with the expected sequence of Bann-RBD within the context of the *P. pastoris* proteome.

Size assesment by DLS

Bann-RBD in a 10 mM Tris-HCl buffer at pH 7.4 was incubated at 4 °C for 12 h before DLS measurements. The measurements were conducted using a Zetasizer Nano ZS instrument (Malvern, Worcestershire, UK) at 25 °C with an incident He–Ne laser (633 nm). This experiment was carried out at PT Bio Farma (Persero) Indonesia. The particle size distribution was recorded, and the data were analyzed using the software provided by Malvern within the instrument.

For TEM observation, a 5 µL aliquot of Bann-RBD in 10 mM Tris-HCl buffer at pH 7.4 was applied to hydrophilized carbon-coated Cu-grid, left for 60 s, and then removed. Subsequently, a drop of 5 µL of aqueous 2% w/v tungstophosphoric acid hydrate (Merck) staining was placed on the grid, left for 60 s, and then removed. The grid was washed with ddH_2O. The sample-loaded carbon-coated grids were allowed to dry for 30 min and

were then subjected to TEM observation using a TALOS F200C instrument (Thermo Scientific, USA) with an acceleration voltage of 200 kV. This experiment was conducted at *Badan Riset dan Inovasi Nasional* (BRIN) Indonesia.

Antigenicity study of Bann-RBD

Indirect ELISA experiments were conducted to assess the interaction of Bann-RBD with specific antibodies. Ninety-six-well ELISA plates (514201, NEST) were coated with 1 µg/mL of Bann-RBD protein or commercial RBD protein (FPZ0648, Fapon) was used as a positive control in 50 mM carbonate-bicarbonate buffer pH 9.6 coating buffer per well, incubating overnight at 4 °C. Negative controls 1 µg/mL human serum albumin (Sigma) in coating buffer were also incubated overnight. The following day, the plates were washed with PBS with 0.1% (v/v) Tween-20, or PBS-T, and blocked with 0.1% BSA (126593-10GM Merck, Merck Millipore) in PBS-T for 1 h at room temperature.

Monoclonal human anti SARS-CoV-2 spike-S1 IgG (A02038-1, GenScript) served as the primary antibody and was incubated for 2 h at room temperature. After washing, HRP conjugated goat anti-human IgG (GenScript) was used as the secondary antibody. Plates were incubated for 1 h at room temperature before washing, followed by the addition of 3,3',5,5'-tetramethylbenzidine (TMB) substrate (34028, Thermo Scientific). Plates were incubated for 5 min in dark until a blue color was observed. After incubation, the reaction was stopped by adding 2 M H_2SO_4, which resulted in the solution turning yellow. The absorbance at a wavelength of 450 nm was measured using a microplate reader (SpectraMax ABS Plus). Triplicate values of raw data from the OD_{450} were averaged. The titer cutoff value was calculated as threefold mean of negative controls.

Mouse immunization studies

Male and female 6 weeks old BALB/c mice (PT BMTI, Indonesia) were used for immunization to test the immunogenicity of Bann-RBD vaccines ($n=6$ for each group). All methods were carried out in accordance with relevant guidelines and regulations. Animal experiments were approved by the Animal Research Ethics Committee of Bandung Institute of Technology (Ethical Approval Number: KEP/1/2024/II/H221223OJ/ITRM). The mice were housed with a 12-hour dark-light cycle and provided access to water and feed *ad libitum*. Same sex and group of mice were housed together in individually ventilated cages with three or four mice per cage. All methods are reported in accordance with ARRIVE guidelines (https://arriveguidelines.org)[65].

Immunization was carried out intramuscularly on primary vaccination and two boosters, with a three weeks (21 days) interval between vaccinations. The mice were vaccinated with 10 µg Bann-RBD containing alhydrogel 1.3% (v/v) and 10 µg CpG (ODN 2395 VacciGrade, InvivoGen). As negative controls mice were vaccinated with adjuvant alhydrogel 1.3% (v/v) and 10 µg CpG in PBS; adjuvant alhydrogel 1.3% (v/v) in PBS; and PBS only. Three weeks after the second booster (63 days after initial immunization), the animals were sacrificed by CO_2 gas euthanasia using a gradual fill method in a chamber that less likely to cause pain according to AVMA Guidelines for the Euthanasia of Animals[66].

The blood samples were collected from retro-orbital bleeding on days 0, 7, 14, 21, 42, and 63 after first vaccination. Mice sera were prepared by incubated the blood samples on ice for 2 h or until coagulated, centrifugated at 2800 g for 10 min at 4 °C, and separated the sera. Mice sera were stored at − 80 °C for further analysis.

Immune response analysis in mice

Indirect ELISA tests were performed to analyze the specific antibodies in mice sera. Ninety-six-well ELISA plates were coated with 1 µg/mL of Bann-RBD protein in 50 mM carbonate-bicarbonate buffer pH 9.6 coating buffer per well, then incubated overnight at 4 °C. Negative controls were included using coating buffer without Bann-RBD protein were also incubated overnight. The following day, the plates were washed with PBS with 0.1% (v/v) Tween-20, or PBS-T, and blocked with 0.1% BSA in PBS-T for 1 h at room temperature. Mice sera with PBS-diluted at a ratio of 1:1000 were served as the primary antibody and incubated for 2 h at room temperature. Subsequently after washing, HRP conjugated goat anti-mouse IgG (W4021, Promega) was used as the secondary antibody. Plates were incubated for 1 h at room temperature before washing, followed by the addition of TMB substrate. Plates were incubated for 5 min in the dark until a blue color was observed. After incubation, the reaction was stopped by adding 2 M H_2SO_4, causing the solution to change to a yellow color. The absorbance at a wavelength of 450 nm was measured using a microplate reader. Triplicate values of raw data from the OD_{450} were averaged. Statistical analysis was performed between groups with multiple time points using two-way ANOVA with Tukey's multiple comparison post hoc test.

The interaction between mouse IgG-specific antibodies and the commercial SARS-CoV-2 spike-S1 protein (Z03501-100, GenScript) was studied using a similar procedure. Microplates were coated with 1 µg/mL of SARS-CoV-2 spike-S1 protein in a coating buffer and incubated overnight at 4 °C. This was followed by the same protocol to analyze the immune response in mice sera.

Detection of anti-SARS-CoV-2 neutralizing antibodies

Specific anti-SARS-CoV-2 neutralizing antibodies in mice sera were detected using a commercial SARS-CoV-2 neutralization antibody ELISA kit (Elabscience). The kit designed to quantifies anti-SARS-CoV-2 RBD neutralizing antibodies (NAbs) that are able to block the interaction between RBD and ACE-2. The neutralization antibody ELISA kit was used according to the manufacturer's instructions. Mice sera from male and female mice, collected 21 days after the second booster, were tested. The groups included sera from mice boosted with either Bann-RBD formulated with alhydrogel 1.3% (v/v) and 10 µg CpG; alhydrogel 1.3% (v/v) combined with 10 µg CpG in PBS; or alhydrogel 1.3% (v/v) in PBS. The sera were diluted 10-fold using sample diluent. The standard working solution, positive and negative controls were diluted according to the manual using the

reference standard diluent. The positive control consists of serum obtained from individuals who have received the COVID-19 vaccine, while the negative control from the kit uses serum from healthy volunteers who have neither been vaccinated nor exposed to COVID-19 infection.

Next, 50 µL of each standard, pre-treated sera sample, and control dilution were added to the microtiter plate that already immobilized with ACE-2, followed by the immediate addition of HRP-conjugated RBD. The plate was then covered and incubated at 37 °C for 60 min, after which it was washed three times. Substrate reagent was added to each well and incubated in the dark for 15 min at 37 °C. The reaction was stopped by adding the stop solution, and the absorbance was measured at 450 nm using a microplate reader. If the sample contains neutralizing antibodies, they will prevent the RBD from interacting with recombinant ACE-2, leading to a reduction in the optical density signal.

Preliminary toxicity and safety studies

We conducted initial toxicity studies of the vaccine injection through various methods. The toxicity of the Bann-RBD protein sequence was assessed in silico using the web-based ToxinPred2 server (https://webs.iiitd.edu.in/raghava/toxinpred2/index.html)[67]. Local reactogenicity at the injection site was observed using the Draize test based on the appearance of edema and erythema after each injection in mice. We monitored the body weight daily and measured the body temperature at the ear 1, 2, and 24 h post-injection using an infrared thermometer (OEM, China).

Data availability

All data generated or analysed during this study are included in this published article and its supplementary information files.

Received: 1 December 2024; Accepted: 5 May 2025
Published online: 27 May 2025

References

1. WHO. Statement on the fifteenth meeting of the IHR (2005) Emergency Committee on the COVID-19 pandemic. (2023). https://www.who.int/news/item/05-05-2023-statement-on-the-fifteenth-meeting-of-the-international-health-regulations-%282005%29-emergency-committee-regarding-the-coronavirus-disease-%28covid-19%29-pandemic
2. Chen, W. H. et al. Yeast-expressed Recombinant SARS-CoV-2 receptor binding domain RBD203-N1 as a COVID-19 protein vaccine candidate. *Protein Expr Purif.* **190** (2022).
3. WHO. COVID-19 vaccine tracker and landscape. (2023). https://www.who.int/publications/m/item/draft-landscape-of-covid-19-candidate-vaccines
4. Smith, K. et al. Safety of the NVX-CoV2373 COVID-19 vaccine in randomized placebo-controlled clinical trials. *Vaccine* **41**, 3930–3936 (2023).
5. Gao, L. et al. Safety and immunogenicity of a protein subunit COVID-19 vaccine (ZF2001) in healthy children and adolescents aged 3–17 years in China: A randomised, double-blind, placebo-controlled, phase 1 trial and an open-label, non-randomised, non-inferiority, phase 2 trial. *Lancet Child. Adolesc. Health*. **7**, 269–279 (2023).
6. Chavda, V. P., Vora, L. K. & Vihol, D. R. COVAX-19® Vaccine: Completely blocks virus transmission to non-immune individuals. *Clin. Complement. Med. Pharmacol.* **1**, (2021).
7. Lin, Y. J. et al. Protection of hamsters challenged with SARS-CoV-2 after two doses of MVC-COV1901 vaccine followed by a single intranasal booster with nanoemulsion adjuvanted S-2P vaccine. *Sci. Rep.* **12**, (2022).
8. Thuluva, S. et al. Evaluation of safety and immunogenicity of receptor-binding domain-based COVID-19 vaccine (Corbevax) to select the optimum formulation in open-label, multicentre, and randomised phase-1/2 and phase-2 clinical trials. *EBioMedicine* **83**, (2022).
9. Frederiksen, L. S. F., Zhang, Y., Foged, C. & Thakur, A. The Long Road Toward COVID-19 herd immunity: Vaccine platform technologies and mass immunization strategies. *Front. Immunol.* **11** (2020).
10. Jackson, C. B., Farzan, M., Chen, B. & Choe, H. Mechanisms of SARS-CoV-2 entry into cells. *Nat. Rev. Mol. Cell Biol.* **23**, 3–20 (2022).
11. Creech, C. B., Walker, S. C. & Samuels, R. J. SARS-CoV-2 vaccines. *JAMA* **325**, 1318–1320 (2021).
12. Yang, J. et al. A vaccine targeting the RBD of the S protein of SARS-CoV-2 induces protective immunity. *Nature* **586**, 572–577 (2020).
13. Dai, L. & Gao, G. F. Viral targets for vaccines against COVID-19. *Nat. Rev. Immunol.* **21**, 73–82 (2021).
14. Kelly, H. G. et al. Self-assembling influenza nanoparticle vaccines drive extended germinal center activity and memory B cell maturation. *JCI Insight* **5**, (2020).
15. Zang, J. et al. Yeast-produced RBD-based recombinant protein vaccines elicit broadly neutralizing antibodies and durable protective immunity against SARS-CoV-2 infection. *Cell. Discov.* **7** (2021).
16. Routhu, N. K. et al. SARS-CoV-2 RBD trimer protein adjuvanted with Alum-3 M-052 protects from SARS-CoV-2 infection and immune pathology in the lung. *Nat. Commun.* **12**, (2021).
17. Argentinian AntiCovid Consortium. Covalent coupling of Spike's receptor binding domain to a multimeric carrier produces a high immune response against SARS-CoV-2. *Sci. Rep.* **12**, 692 (2022).
18. Lainšček, D. et al. A nanoscaffolded spike-RBD vaccine provides protection against SARS-CoV-2 with minimal anti-scaffold response. *Vaccines* **9**, 431 (2021).
19. Matsuura, K. Dressing up artificial viral capsids self-assembled from C-terminal-modified β-annulus peptides. *Polym. J.* **52**, 1035–1041 (2020).
20. Matsuura, K., Watanabe, K., Matsuzaki, T., Sakurai, K. & Kimizuka, N. Self-assembled synthetic viral capsids from a 24-mer viral peptide fragment. *Angew. Chem. Int. Ed.* **49**, 9662–9665 (2010).
21. Kanekiyo, M. & Buck, C. B. Virus-Like particle and nanoparticle vaccines. In Human Vaccines: Emerging Technologies in Design and Development 87–98 (Elsevier Inc., 2017)
22. Wichgers Schreur, P. J. et al. Vaccine efficacy of self-assembled multimeric protein scaffold particles displaying the glycoprotein Gn head domain of rift Valley fever virus. *Vaccines* **9**, 301 (2021).
23. Kumar, R. & Kumar, P. Yeast-based vaccines: New perspective in vaccine development and application. *FEMS Yeast Res.* **19** (2019).
24. Rachman, E. A. G. et al. Construction, expression and characterization of multi cassettes encoding Indonesian small hepatitis B surface antigen (s-HBsAg) in methylotropic yeast *Pichia pastoris*. *Biotechnology* **14**, 225–232 (2015).

25. Karbalaei, M., Rezaee, S. A. & Farsiani, H. *Pichia pastoris*: A highly successful expression system for optimal synthesis of heterologous proteins. *J. Cell. Physiol.* **235**, 5867–5881 (2020).
26. Consortium, A. A. Structural and functional comparison of SARS-CoV-2-spike receptor binding domain produced in *Pichia pastoris* and mammalian cells. *Sci. Rep.* **10**, (2020).
27. Matsuura, K., Watanabe, K., Matsushita, Y. & Kimizuka, N. Guest-binding behavior of peptide nanocapsules self-assembled from viral peptide fragments. *Polym. J.* **45**, 529–534 (2013).
28. Harrison, S. C. W. F. B. G. Tomato bushy stunt virus at 2.9 Å resolution. *Nature* **276**, 368–373 (1978).
29. Hopper, P., Harrison'And, S. C. & Sauer', R. T. Structure of tomato bushy stunt virus coat protein sequence determination and its structural implications. J. *Mol. Biol* **177**, 701–713 (1984).
30. Rajib, M. S. A., Hossain, M. B., Satou, Y. & Ikeda, T. Surface glycoprotein [Severe acute respiratory syndrome coronavirus 2] - Protein - NCBI. (2021). https://www.ncbi.nlm.nih.gov/protein/UAL04647.1
31. Mirdita, M. et al. ColabFold: Making protein folding accessible to all. *Nat. Methods*. **19**, 679–682 (2022).
32. Montiel-Garcia, D. et al. VIPERdb v3.0: A structure-based data analytics platform for viral capsids. *Nucleic Acids Research*. **49**, D809–D816 (2021).
33. Jespersen, M. C., Peters, B., Nielsen, M. & Marcatili, P. BepiPred-2.0: Improving sequence-based B-cell epitope prediction using conformational epitopes. *Nucleic Acids Res.* **45**, W24–W29 (2017).
34. Lundegaard, C., Lund, O. & Nielsen, M. Accurate approximation method for prediction of class I MHC affinities for peptides of length 8, 10 and 11 using prediction tools trained on 9mers. *Bioinformatics* **24**, 1397–1398 (2008).
35. Jensen, K. K. et al. Improved methods for predicting peptide binding affinity to MHC class II molecules. *Immunology* **154**, 394–406 (2018).
36. Honorato, R. et al. The HADDOCK2.4 web server for integrative modeling of biomolecular complexes. *Nat. Protoc.* **19**, 3219–3241 (2024).
37. Honorato, R. V. et al. Structural biology in the clouds: The WeNMR-EOSC ecosystem. *Front. Mol. Biosci.* **8** (2021).
38. Xue, L. C. et al. PRODIGY: A web server for predicting the binding affinity of protein-protein complexes. *Bioinformatics* **32**, 3676–3678 (2016).
39. Vangone, A. & Bonvin, A. M. Contacts-based prediction of binding affinity in protein–protein complexes. *Elife* **4**, (2015).
40. Gasteiger, E. et al. *Protein Identification and Analysis Tools on the ExPASy Server* (Springer, 1999).
41. Liu, L. et al. Potent neutralizing antibodies against multiple epitopes on SARS-CoV-2 Spike. *Nature* **584**, 450–456 (2020).
42. Liu, Y. et al. A vaccine based on the yeast-expressed receptor-binding domain (RBD) elicits broad immune responses against SARS-CoV-2 variants. *Front. Immunol.* **13** (2022).
43. Dai, L. et al. A universal design of betacoronavirus vaccines against COVID-19, MERS, and SARS. *Cell* **182**, 722–733e11 (2020).
44. Ma, X. et al. Nanoparticle vaccines based on the receptor binding domain (RBD) and heptad repeat (HR) of SARS-CoV-2 elicit robust protective immune responses. *Immunity* **53**, 1315–1330e9 (2020).
45. Inaba, H. & Matsuura, K. Functional peptide nanocapsules self-assembled from β-annulus peptides. *Methods Mol. Biol.* **2208**, 101–121 (2021).
46. Peters, B., Nielsen, M. & Sette, A. T. Cell epitope predictions. *Annu. Rev. Immunol.* **38**, 123–145 (2020).
47. Jiang, M. et al. Epitope profiling reveals the critical antigenic determinants in SARS-CoV-2 RBD-Based antigen. *Front. Immunol.* **12**, (2021).
48. Li, S. et al. Immunodominance of epitopes and protection ecacy of RBD antigen are differentially altered by different adjuvants and immune routes. (2022).
49. Sidney, J., Peters, B. & Sette, A. Epitope prediction and identification- adaptive T cell responses in humans. *Seminars Immunol.* **50** (2020).
50. Pino, M. et al. A yeast-expressed RBD-based SARS-CoV-2 vaccine formulated with 3 M-052-Alum adjuvant promotes protective efficacy in non-human primates. *Sci. Immunol.* **6** (2021).
51. Chen, W. H. et al. Genetic modification to design a stable yeast-expressed recombinant SARS-CoV-2 receptor binding domain as a COVID-19 vaccine candidate. *Biochim. Biophys. Acta Gen. Subj.* **1865** (2021).
52. Pollet, J. et al. SARS-CoV-2 RBD219-N1C1: A yeast-expressed SARS-CoV-2 recombinant receptor-binding domain candidate vaccine stimulates virus neutralizing antibodies and T-cell immunity in mice. *Hum. Vaccin. Immunother.* **17**, 2356–2366 (2021).
53. Chen, W. H. et al. Yeast-expressed SARS-CoV recombinant receptor-binding domain (RBD219-N1) formulated with aluminum hydroxide induces protective immunity and reduces immune enhancement. *Vaccine* **38**, 7533–7541 (2020).
54. Newby, M. L., Allen, J. D. & Crispin, M. Influence of glycosylation on the immunogenicity and antigenicity of viral immunogens. *Biotechnol. Adv.* **70** (2024).
55. Luping Zheng, Y. M. M. C. G. W. C. Y. X.-E. Z. SARS-CoV-2 Spike protein receptor-binding domain N-glycans facilitate viral internalization in respiratory epithelial cells. *Biochem. Biophys. Res. Commun.* **579**, 69–75 (2021).
56. Matsuura, K. & Honjo, T. Artificial viral capsid dressed up with human serum albumin. *Bioconjug. Chem.* **30**, 1636–1641 (2019).
57. Fujita, S. & Matsuura, K. Self-Assembled artificial viral capsids bearing coiled-coils at the surface. *Org. Biomol. Chem.* **15**, 5070–5077 (2017).
58. Nakamura, Y., Yamada, S., Nishikawa, S. & Matsuura, K. DNA-modified artificial viral capsids self-assembled from DNA-conjugated β-annulus peptide. *J. Pept. Sci.* **23**, 636–643 (2017).
59. Matsuura, K., Ueno, G. & Fujita, S. Self-assembled artificial viral capsid decorated with gold nanoparticles. *Polym. J.* **47**, 146–151 (2015).
60. Furukawa, H. et al. Enveloped viral replica equipped with Spike protein derived from SARS-CoV-2. *ACS Synth. Biol.* **13**, 2029–2037 (2024).
61. Pollet, J. et al. Receptor-binding domain recombinant protein on alum-CpG induces broad protection against SARS-CoV-2 variants of concern. *Vaccine* **40**, 3655–3663 (2022).
62. The Jackson Laboratory. Body Weight Information for BALBc at the Jackson Laboratory. (2025). https://www.jax.org/jax-mice-and-services/strain-data-sheet-pages/body-weight-chart-000651
63. Lee, C. T., Zhong, L., Mace, T. A. & Repasky, E. A. Elevation in body temperature to fever range enhances and prolongs subsequent responsiveness of macrophages to endotoxin challenge. *PLoS ONE* **7**, (2012).
64. DeLano, W. L. & Bromberg, S. PyMOL User's Guide. (2004).
65. du Sert, N. et al. (ed, P.) Reporting animal research: Explanation and elaboration for the arrive guidelines 2.0. *PLoS Biology* **18**, (2020).
66. Leary, S. et al. *AVMA Guidelines for the Euthanasia of Animals* (American Veterinary Medical Association, 2013).
67. Sharma, N., Naorem, L. D., Jain, S. & Raghava, G. P. S. ToxinPred2: An improved method for predicting toxicity of proteins. *Brief. Bioinform* **23**, (2022).

Acknowledgements

The authors thank PT Bio Farma (Persero) for their kindness in using their DLS instrument and to BRIN for TEM analysis. LC-MS/MS study used NCRIS-enabled Australian Proteome Analysis Facility (APAF) infrastructure.

Author contributions

O.J. performed the experiments, analyzed the data, and prepared the manuscript. M.D.F., A.D. and F.P. performed the experiments. S.D.K, and F.F.M. analyzed the data. E.G.R., M.I.T., and A.A.A. analyzed the data and revised the manuscript. I. and K.V. conceived the ideas, designed the experiments, supervised, analyzed and validated the data prepared and revised the manuscript. D.N. conceived the ideas, designed the experiments, supervised, analyzed and validated the data, provided resources, managed the research project, and prepared, revised, and submitted the manuscript. All authors have read and agreed to the final version of the manuscript.

Funding

This work was funded by 2023 P2MI-FMIPA Institut Teknologi Bandung and Indonesia Toray Science Foundation (ITSF) Science and Technology Research Grant.

Declarations

Competing interests

The authors declare no competing interests.

Additional information

Supplementary Information The online version contains supplementary material available at https://doi.org/10.1038/s41598-025-01242-5.

Correspondence and requests for materials should be addressed to D.N.

Reprints and permissions information is available at www.nature.com/reprints.

Publisher's note Springer Nature remains neutral with regard to jurisdictional claims in published maps and institutional affiliations.